The EMBO Journal Vol.19 No.1 pp.103–113, 2000

A conformational switch controlling HIV-1 morphogenesis

Ingolf Gross, Heinz Hohenberg, Thomas Wilk[1], Klaus Wiegers, Mira Grättinger, Barbara Müller, Stephen Fuller[1] and Hans-Georg Kräusslich[2]

Heinrich-Pette-Institut für experimentelle Virologie und Immunologie an der Universität Hamburg, Martinistrasse 52, D-20251 Hamburg and [1]European Molecular Biology Laboratory, D-69017 Heidelberg, Germany

[2]Corresponding author
e-mail: hgk@hpi.uni-hamburg.de

Assembly of infectious human immunodeficiency virus type 1 (HIV-1) proceeds in two steps. Initially, an immature virus with a spherical capsid shell consisting of uncleaved Gag polyproteins is formed. Extracellular proteolytic maturation causes rearrangement of the inner virion structure, leading to the conical capsid of the infectious virus. Using an *in vitro* assembly system, we show that the same HIV-1 Gag-derived protein can form spherical particles, virtually indistinguishable from immature HIV-1 capsids, as well as tubular or conical particles, resembling the mature core. The assembly phenotype could be correlated with differential binding of the protein to monoclonal antibodies recognizing epitopes in the HIV-1 capsid protein (CA), suggesting distinct conformations of this domain. Only tubular and conical particles were observed when the protein lacked spacer peptide SP1 at the C-terminus of CA, indicating that SP1 may act as a molecular switch, whose presence determines spherical capsid formation, while its cleavage leads to maturation.
Keywords: assembly/Gag/HIV-1/maturation/retrovirus

Introduction

Virus particles are highly organized assemblies built to package and protect the viral genome, to facilitate entry into the host cell, and to control release and activation of the genome early in infection. Owing to their limited coding capacity, viruses have evolved strategies of genetic economy and in many cases encode only a single structural protein, forming the capsid shell. Consequently, viral capsid assembly and maturation are tightly controlled processes following an ordered multi-step pathway. A simple and efficient way to regulate the properties of the protein shell is the controlled conformational transition of capsomer subunits. Subtle differences of individual protomers and temporally regulated structural alterations can act as molecular switches to determine the morphology of the assembling particle and to promote rearrangements in capsid architecture, thereby stabilizing or destabilizing the particle in an ordered fashion. Studies on icosahedral capsids have shown that conformational flexibility is indeed required to form a complex structure from chemically identical subunits, and coat proteins must adopt distinct conformations to allow for geometrically different interactions with neighboring subunits (reviewed by Johnson and Speir, 1997). Usually, the core of the protein is stable and variability is accomplished by alteration of flexible regions often located near the N- or C-terminus of the protein. In the case of polyoma viruses, a long C-terminal arm emerges at different angles from the coat protein and acts as a flexible connector, resulting in different geometries of intersubunit contacts (Liddington *et al*., 1991). This allows the formation of icosahedral particles of various sizes as well as tubular particles from the same pentameric building block. A structurally well characterized example for temporal conformational changes of a viral shell protein is the maturation of phage P22 from empty procapsids into stable capsids. This involves a large hinge movement between coat protein domains resulting in the linkage of neighboring capsomers (Prasad *et al*., 1993; Prevelige *et al*., 1993).

The protective shells of retroviruses like human immunodeficiency virus type 1 (HIV-1) are more complex than icosahedral capsids, but it seems likely that similar principles of conformational control also apply in this case. Mature HIV-1 particles contain their genome as a condensed ribonucleoprotein (RNP) core encased in a proteinaceous cone-shaped capsid shell and surrounded by a lipid bilayer derived from the host cell (Nermut and Hockley, 1996). Initially, they are released as immature particles containing a spherical shell of structural polyproteins (Gag) underneath the virion membrane. Gag alone is capable of organizing the formation and release of virus-like particles (Gheysen *et al*., 1989). Cryo-electron microscopy (EM) analysis of HIV-1 and murine leukemia virus particles revealed that immature capsids do not display icosahedral symmetry, but Gag molecules are arranged with local order in spherical assemblies (Fuller *et al*., 1997; Yeager *et al*., 1998). Virions subsequently undergo a proteolytic maturation step, which is essential for infectivity and leads to condensation of the inner core and capsid shell. Maturation probably serves to convert the stable immature capsid shell into a metastable mature core, ready for uncoating. Thereby, it switches the virion from an 'assembly mode' to a 'disassembly mode'. Mutational analysis indicated that HIV-1 maturation follows an ordered pathway of sequential cleavages, controlled by the rate of proteolysis at individual sites (Wiegers *et al*., 1998). The HIV-1 Gag polyprotein is cleaved by the virus-encoded proteinase (PR) into the functional products matrix (MA), which lines the inner face of the membrane, capsid (CA), which forms the cone-shaped capsid shell, nucleocapsid (NC), which binds and condenses the viral genome, and p6, which is involved in virion release (Figure 1). Two short spacer peptides SP1 and SP2 separate

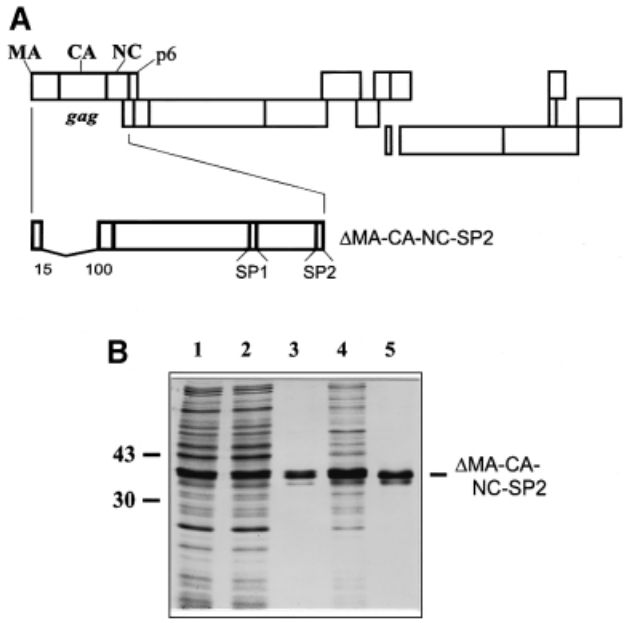

Fig. 1. Expression and purification of the ΔMA-CA-NC-SP2 protein. (**A**) Schematic representation of the HIV-1 specific sequences encoded in the expression plasmid. At the top, the coding region of the HIV-1 genome is shown, with open reading frames depicted as boxes. The domains of the *gag* reading frame are identified. The HIV-specific region encoded by plasmid pET ΔMA-CA-NC-SP2 is expanded below. The numbers indicate the amino acids of MA flanking the deletion. (**B**) Coomassie Blue-stained SDS–polyacrylamide gel representing purification of ΔMA-CA-NC-SP2. Lanes: 1, lysate of induced bacteria; 2 and 3, soluble and insoluble material after centrifugation at intermediate speed; 4, material after ammonium sulfate precipitation and anion exchange chromatography; 5, purified protein after cation exchange chromatography. The protein migrating slightly faster than ΔMA-CA-NC-SP2 corresponds to a C-terminally truncated form that is probably cleaved in the NC domain by a bacterial protease. Molecular mass standards (in kDa) are indicated on the left, the position of ΔMA-CA-NC-SP2 is marked on the right.

the CA and NC and the NC and p6 domains, respectively, and are also released by proteolytic cleavages (Henderson *et al*., 1990).

The determination of three-dimensional structures of individual domains of the HIV-1 Gag protein (Massiah *et al*., 1994; Matthews *et al*., 1995; Gitti *et al*., 1996; Momany *et al*., 1996; Gamble *et al*., 1997; De Guzman *et al*., 1998; Berthet-Colominas *et al*., 1999) led to a better understanding of functionally important features of these proteins, but did not elucidate the structural principles governing particle assembly and maturation. A high resolution structure of assembled particles, defining important intermolecular interactions, is not available to date. With the aim of characterizing the formation, maturation and architecture of HIV particles in greater detail, we and others have applied *in vitro* assembly systems using purified HIV-1 Gag-derived proteins. These studies demonstrated that the CA domain alone or attached to the nucleic acid binding NC domain produces tubular particles with helical symmetry, resembling the mature capsid (Campbell and Vogt, 1995; Gross *et al.*, 1997; von Schwedler *et al*., 1998; Ganser *et al*., 1999). Addition of as little as four amino acids to the N-terminus of CA abolished tube formation and some N-terminally extended versions arranged to spherical particles of heterogeneous size in the *in vitro* system (Gross *et al*., 1998; von Schwedler *et al*., 1998; Campbell and Rein, 1999). However, none of these *in vitro* assembled particles truly resembled the immature HIV virion.

The observation that tube formation is prevented by N-terminal extensions of CA led to the proposition that HIV-1 capsid maturation is induced by proteolytic cleavage between MA and CA, allowing the N-terminus of CA to refold into a β-hairpin structure, hypothesized to be part of a CA–CA interface characteristic of the mature particle (von Schwedler *et al*., 1998). On the other hand, mutational analyses in the context of the virus indicated that proteolytic liberation of the CA C-terminus from the adjacent SP1 region is also important for particle maturation. Based on molecular modeling, the C-terminus of CA and adjacent SP1 residues have been proposed to form a continuous α-helix (Accola *et al*., 1998), while this region was disordered in the structures of CA determined to date (Gamble *et al*., 1996; Berthet-Colominas *et al*., 1999; Worthylake *et al*., 1999). It appears likely, however, that this region and its non-covalent interactions with other parts of CA or Gag play an important role in determining capsid shape and in regulating maturation.

Forming HIV-1 Gag-derived particles with 'mature' and 'immature' morphology *in vitro* would offer an opportunity to determine whether the morphology of these particles can be correlated to distinct conformational differences in the CA domain, which would probably reflect alterations occurring during maturation. Whereas in the virion the breaking of interdomain interactions and the liberation of new N- and C-terminal residues by proteolytic separation of Gag domains is most likely to be the reason for conformational transitions, *in vitro*, changes in assay conditions may have the same effect. Here, we show that in an *in vitro* assembly system, the same HIV-1 Gag-derived protein can form spherical particles, virtually indistinguishable from immature HIV-1 capsids, as well as tubular or conical particles, resembling the mature core. This switch of assembly phenotype could be correlated with differential binding of the protein to monoclonal antibodies (mAbs), suggesting conformational transitions in the CA domain. A similar protein lacking SP1, on the other hand, only assembled into short tubes and cones.

Results

In vitro assembly of ΔMA-CA-NC-SP2 yields spherical particles closely resembling immature HIV-1 cores

Previously, we had shown that a large deletion removing the globular part of the HIV-1 MA domain (ΔMA) in the context of an infectious proviral clone alters the budding site of the virus, but does not detectably change the morphology of resulting virions (Fäcke *et al*., 1993). *In vitro* assembly of an HIV-1 Gag-derived protein containing the MA and CA domains with the same deletion from amino acid 16 to 99 of MA (ΔMA-CA), on the other hand, yielded spherical particles of variable size but considerably smaller than authentic immature HIV-1 cores (Gross *et al*., 1998). In order to analyze whether the presence of additional segments of HIV-1 Gag makes *in vitro* assembled particles more akin to immature cores, we constructed the bacterial expression plasmid pET

ΔMA-CA-NC-SP2, which encodes an HIV-1 Gag-derived protein lacking amino acids 16–99 of MA and the C-terminal p6 domain (Figure 1A). The specific product accumulated to ~10% of total bacterial protein following induction of *Escherichia coli* BL21 DE3 cells (Figure 1B, lane 1), and was purified by differential ammonium sulfate precipitation and cation exchange chromatography (Figure 1B). Approximately 2–5 mg of recombinant protein at >90% purity were obtained per liter of induced bacterial culture (Figure 1B, lane 5).

In vitro assembly was performed by dialysis of ΔMA-CA-NC-SP2 (2 mg/ml) for 2 h against pH 8.0 buffer containing 0.1 M salt in the presence of a 73mer oligodeoxynucleotide. Previously, it had been shown that single-stranded DNA oligonucleotides can substitute for RNA in *in vitro* assembly experiments (Campbell and Rein, 1999). Assembly products were analyzed by negative stain EM, revealing spherical structures of regular morphology with a homogeneous size distribution as well as amorphous protein aggregates (data not shown). In an attempt to remove aggregates and enrich for spherical particles, we performed consecutive centrifugation in the microcentrifuge for 5 and 60 min. Unexpectedly, virtually all spheres were found in the pellet fraction after 5 min centrifugation, most likely due to their reversible aggregation. These particles were very regular in size and morphology with an external diameter of 90 nm (±5 nm) and a wall thickness of 15 nm on negative stain EM (Figure 2A and B). Most particles were not completely closed but contained a small gap (Figure 2A). Approximately 30% of the ΔMA-CA-NC-SP2 protein used for *in vitro* assembly was found in the particle fraction. Subsequent centrifugation of the supernatant for 60 min led to sedimentation of a further 30% of input protein, but virtually no regular particles were detected in this fraction or in the remaining supernatant (data not shown).

Thin section EM analysis of spherical particles confirmed their regularity and homogeneous size distribution with an external diameter of 80–85 nm (Figure 2C). The size difference compared with negatively stained specimens is probably due to shrinkage during fixation and dehydration. The *in vitro* assembled particles closely resembled immature HIV-1 virions produced from an infected T-cell line in the presence of an inhibitor of HIV-1 PR (Figure 2E). Stereo images of ΔMA-CA-NC-SP2 particles revealed hollow spheres that were not collapsed but retained their three-dimensional architecture (Figure 2C and D). Particles shown in the stereo image were sectioned either through the concave (particle 1) or convex cap (particle 2) or through the center of the sphere (particle 3), the latter yielding the typical electron-dense ring structure (Figure 2C and D).

Similar results were obtained when single-stranded oligodeoxynucleotides of 92, 73, 55 or 31 nucleotides and of different sequence were applied. The efficiency of *in vitro* assembly was reduced for a 16mer oligodeoxynucleotide and no spheres were detected when a 12mer was used (data not shown). *In vitro* assembly was optimal at molar ratios of protein:nucleic acid (73mer) between 5:1 and 16:1, with both higher and lower concentrations of oligodeoxynucleotide leading to gradual loss of assembly. Performing the reaction in the presence of total *E.coli* RNA or of the long single-stranded DNA of bacteriophage M13 (6400 nucleotides) yielded assembly of protein aggregates and incomplete particles (data not shown). Most likely, multiple particles were nucleated on a single molecule of nucleic acid. A similar assembly mode has been suggested previously (Fuller *et al*., 1997). *In vitro* assembly was optimal at a protein concentration of 1–2 mg/ml, but sphere formation could still be detected at a concentration of 0.1 mg/ml (data not shown).

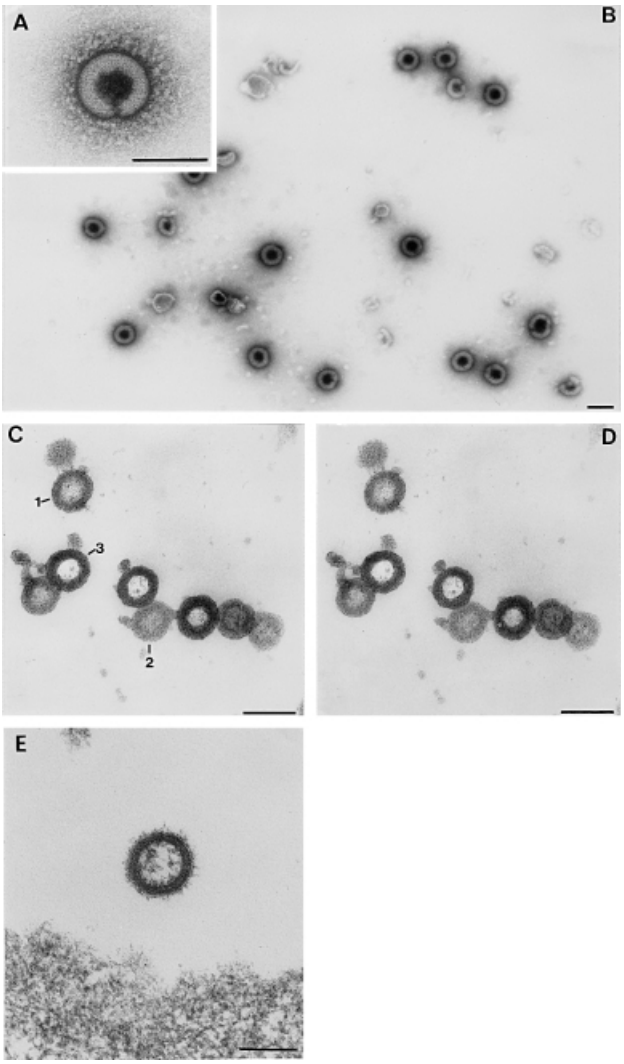

Fig. 2. Electron microscopy analysis of ΔMA-CA-NC-SP2 *in vitro* assembly products. Assembly reactions were performed by dialyzing ΔMA-CA-NC-SP2 for 2 h against 50 mM Tris–HCl pH 8.0, 0.1 M NaCl in the presence of a single-stranded DNA-oligonucleotide (73 nt) at a molar ratio of protein to DNA of 13:1. Subsequently, assembly reactions were centrifuged for 5 min at full speed in an Eppendorf microcentrifuge. (**A** and **B**) Particles were resuspended in dialysis buffer at 1/4 of the original volume and analyzed by negative stain EM. (**C** and **D**) Particles were drawn into capillary tubes and analyzed by ultrathin section EM. Stereo micrographs were taken at an angle of ±6°. Particles designated (1), (2) and (3) are referred to in the text. (**E**) An immature HIV-1 particle obtained from an infected T-cell line in the presence of a specific HIV-1 PR inhibitor and analyzed by ultrathin section EM. Bar, 100 nm.

Cryo-electron microscopy analysis of in vitro assembled spheres

For a detailed comparison of the fine structure of *in vitro* assembled ΔMA-CA-NC-SP2 particles and immature

HIV-1 virions or virus-like particles, we performed cryo-EM on assembly products, obtained by dialysis against pH 8.0 buffer in the presence of a 73mer oligodeoxynucleotide. Cryo-EM avoids fixatives, dehydration and contrasting agents, and permits analysis of the native particle. Defocus phase contrast allows visualization of the unstained structure and reveals the entire sphere in projection. Figure 3A shows three *in vitro* assembled ΔMA-CA-NC-SP2 particles at high magnification (upper two and lower right panels), revealing their substructure. Lateral interactions of proteins in the assembled sphere result in the formation of two protein layers that are separated from each other by a thin space. The protein layer at lower radial position appears darker, presumably due to the presence of nucleic acid at this position. The protein layer at higher radial position is composed of subunits with a rod-like shape, and corresponds to the CA-derived protein layer of immature virions (Fuller *et al*., 1997; Wilk and Fuller, 1999). A remarkably similar arrangement of protein layers is found in virus-like particles obtained after baculovirus-mediated expression of the Gag polyprotein in insect cells (Figure 3A, left lower panel) and in immature HIV-1 (not shown). In contrast to the *in vitro* assembly products, virus-like particles are enveloped by the viral membrane, and the inner leaflet of this membrane is tightly associated with the MA domain of the Gag polyprotein.

The radial arrangement of protein layers in immature HIV-1 and *in vitro* assembled ΔMA-CA-NC-SP2-derived particles is analyzed in detail in Figure 3B. We have used a Fourier–Bessel method to determine the radial density distribution in spherical particles and generated a three-dimensional radial density profile (Fuller *et al*., 1997). The average radial density profile of 10 *in vitro* assembled particles is shown in the upper panel. The comparison with the average radial density profile of 10 immature HIV-1 particles obtained from a T-cell line infected in the presence of an inhibitor of HIV-1 PR (lower panel) demonstrates the strikingly similar organization of the two types of particles. Major differences are only found at high radial position, indicating the presence of the viral membrane in the immature virion. Protein layers are formed by lateral interactions of individual domains, where each domain is separated from the neighboring domain by regions of low density. The layer at lowest radial position is assigned to the NC domain; the neighboring layer at higher radius, corresponding to a double peak, is formed by the CA domain (Figure 3B; Fuller *et al*., 1997; Wilk and Fuller, 1999).

Figure 3C shows a comparison between the diameters of *in vitro* assembled particles and immature HIV-1 virions. *In vitro* assembled ΔMA-CA-NC-SP2-derived particles exhibited a narrow size distribution with an

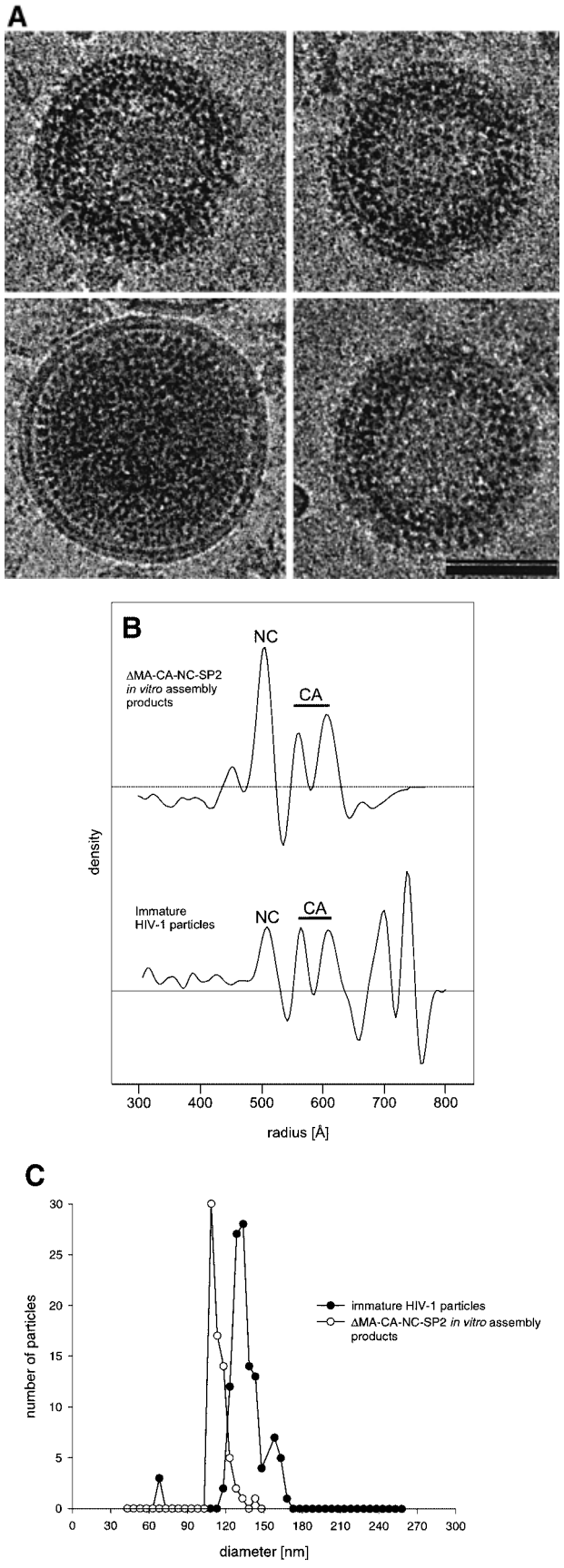

Fig. 3. Cryo-EM analysis of ΔMA-CA-NC-SP2 in *vitro* assembly products. Assembly reactions were performed and particles collected as described in Figure 2. Cryo-EM images (**A**) show the internal organization of *in vitro* assembled particles (upper two panels and lower right panel) and of HIV-like particles produced from baculovirus-infected insect cells (lower left panel). Bar, 100 nm. (**B**) Radial placement of Gag protein domains in ΔMA-CA-NC-SP2 *in vitro* assembly products (upper panel) and in immature HIV-1 virions generated from an infected T-cell line in the presence of PR inhibitor (lower panel). The average radial density profile of 10 particles is shown in both cases. The horizontal axis shows distance in angstroms from the particle center at the left, the vertical axis represents the density of protein layers as a function of mass. (**C**) Size distribution of immature HIV-1 virions (n = 119) and *in vitro* assembled ΔMA-CA-NC-SP2 particles (n = 76).

average diameter of 113.7 nm (±6 nm), while immature virions had a mean diameter of 134.2 nm (±15 nm). This size difference of ~20 nm is mainly due to the lack of the membrane and MA layers in the case of *in vitro* assembly products, which contribute ~10 nm on each side. The similarity in size and radial organization is further supported by the observation that the CA layer, which is shared in both types of particles, is at a radial position of 58.3 nm (±7.5 nm) in immature virus-like particles and at a radial position of 55.8 nm (±3.5 nm) in the case of *in vitro* assembled particles. The *in vitro* assembled particles appeared more regular than virions or virus-like particles and this may reflect the different length of nucleic acid incorporated into the respective particles.

The morphology of in vitro assembly products is dependent on pH

Previous experiments had shown that neutral to slightly alkaline pH is optimal for *in vitro* assembly of regular structures from HIV-1-derived proteins (Campbell and Vogt, 1995; Gross *et al*., 1997), while slightly acidic pH was optimal for Rous sarcoma virus-derived proteins (Campbell and Vogt, 1995). We tested the influence of pH on *in vitro* assembly of ΔMA-CA-NC-SP2 and analyzed the products by negative staining and cryo-EM. Remarkably, dialysis against pH 6.0 buffer abolished sphere assembly and led to efficient formation of hollow tubular particles, which were often closed at one or both ends (Figure 4C and D). Besides tubes, cone-shaped particles resembling the mature HIV-1 core were also produced at this pH (Figure 4C, asterisk). The cylinders were similar to the *in vitro* assembly products of HIV-1 CA and CA-NC (Campbell and Vogt, 1995; Gross *et al*., 1997) with diameters between 40 and 50 nm and variable length. The particle walls were significantly thicker than in the case of CA-derived (15 versus 6 nm; Gross *et al*., 1997) and CA-NC-derived (10 nm) tubes, consistent with the larger mass of the ΔMA-CA-NC-SP2 protein. Thin section EM (Figure 4D) and cryo-EM (data not shown) analysis of pH 6 assembly products also showed tubular and conical particles. Both cones and tubes exhibited a regular substructure and the cones appeared very similar to mature HIV-1 cores and to *in vitro* assembled cones previously described by Ganser *et al*. (1999). The diameters of cylinders analyzed by cryo-EM ranged from 55 to 80 nm. Dimensions of conical particles were more difficult to measure, yielding an approximate length of 145 nm and an approximate width of 35 nm at the narrow end and 75 nm at the broad end.

Different ratios of tubular to spherical particles were observed when assembly was performed by dialysis against pH 7.0 buffer (Figure 4B) or against buffers of pH 6.5 and 7.5 (data not shown), with the relative number of spheres increasing at higher pH values. Only spheres were recovered when the protein was dialyzed against pH 8.0 (Figure 4A), while no ordered structures were formed at pH 9.0. Particles displayed either tubular or spherical morphology, and no particles combining tubular and spherical features were detected. This result suggests that nucleation determines the shape of the particle, and once a tube is initiated, it cannot be extended into a sphere or vice versa. It is important to note that particulate structures were first observed after dialysis for 15 min (data not shown), well before equilibrium with the buffer had been reached. Conceivably, assembly is initiated when the salt concentration in the reaction mixture drops below the threshold for nucleic acid binding. The shape of the resulting particle would then be determined by the pH of the sample at this time, which was found to be ~6.8–7 when the reaction was dialyzed against pH 8 buffer.

To analyze whether the assembly phenotype of ΔMA-CA-NC-SP2 can be altered reversibly, we dialyzed the protein against pH 8 buffer containing high salt to prevent assembly. Subsequently, assembly was initiated by dialysis against pH 8 or 6 low salt buffer in the presence of nucleic acid. Again, only spheres were observed at the high pH and only tubes and cones at the low pH (data not shown). The same result was found when ΔMA-CA-NC-SP2 was predialyzed consecutively against pH 8 and 6 buffers, showing that the protein alteration that determines particle shape is completely reversible. No change in morphology was observed, on the other hand, when assembled spherical or tubular particles were exposed to lower or higher pH, respectively (data not shown).

The assembly phenotype of ΔMA-CA-NC-SP2 is determined by conformational differences

The pH-dependent change in morphology of *in vitro* assembly products suggests that ΔMA-CA-NC-SP2 may have at least two distinct conformations. To determine conformational differences at the molecular level, we analyzed the pH-dependent binding of the protein to HIV-1 CA-specific mAbs. Immune complexes were formed at the respective pH in solution and subsequently captured by polyclonal antiserum against CA and detected with anti-mouse antibodies. Using a panel of CA-specific mAbs, we observed significant pH-dependent differences in binding for antibodies 2.4E6 and 1.5G10, both of which recognized the protein at pH 8 (Figure 5B), but not at pH 6 (Figure 5A), while antibody 3.1B5 was reactive under both conditions. This pH-dependent conformational change was completely reversible, and no reactivity was observed when the protein was first titrated to pH 8 and then back to pH 6 (Figure 5C).

For a more precise determination of the pH inducing the conformational transition, we analyzed the binding of ΔMA-CA-NC-SP2 to mAbs 2.4E6 and 1.5G10 between pH 6 and 8. As shown in Figure 5D, virtually no reactivity was found up to pH 6.8, while efficient binding was seen at pH 7.2. The binding sites of both antibodies detecting conformational differences could be determined using a set of overlapping peptides: antibody 2.4E6 mapped to residues 49–61 and antibody 1.5G10 to residues 109–120 of HIV-1 CA. We hypothesized that antibody binding to the specific peptide epitope, in contrast to binding of the folded protein, might not be pH sensitive. The titration curves shown in Figure 5E (2.4E6) and F (1.5G10) clearly demonstrate pH-independent binding of the respective peptide, indicating that the affinity of the antibody for its epitope is not affected by pH.

Far-UV CD spectra of ΔMA-CA-NC-SP2 recorded at pH 6 and 8 were generally very similar and displayed characteristics of a protein with large α-helical content (data not shown). This result indicates that no major structural rearrangements took place when the pH was altered. At pH 8, a small shift of residual ellipticity to

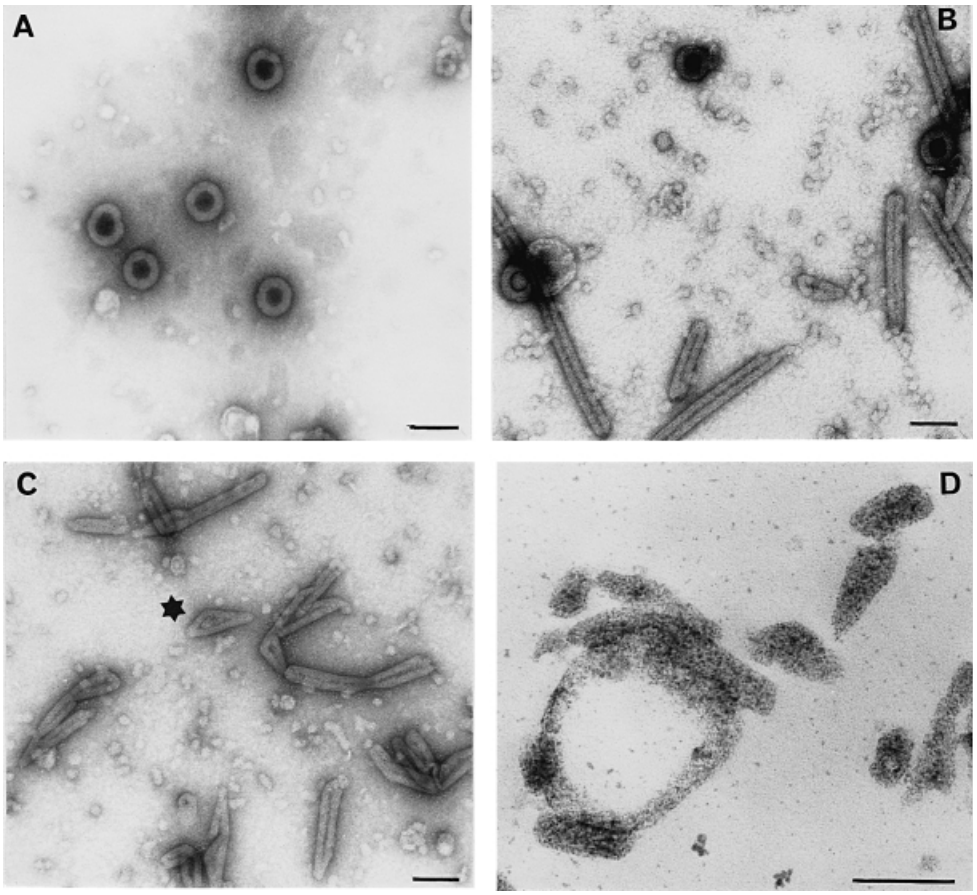

Fig. 4. Analysis of pH-dependent *in vitro* assembly of ΔMA-CA-NC-SP2. Assembly was performed as described in Figure 2, but samples were dialyzed against buffer of either pH 8.0 (**A**), pH 7.0 (**B**) or pH 6.0 (**C** and **D**). Assembly products were concentrated by brief centrifugation and analyzed by negative stain (A–C) or ultrathin section EM (D). The asterisk denotes a cone-shaped particle. Bar, 100 nm.

higher values was observed, which might be due to a slight loss in helicity of the protein.

Deletion of spacer peptide 1 prevents assembly of spherical particles in vitro and inside E.coli cells

The experiments described above showed that ΔMA-CA-NC-SP2 assembles *in vitro* in a conformation-dependent manner into either spheres or tubes and cones, resembling the immature or mature HIV-1 capsid shells, respectively. In contrast, ΔMA-CA and other N-terminally extended versions of CA had previously been shown to form heterogeneous spheres, significantly smaller than authentic immature capsids (Gross *et al*., 1998; von Schwedler *et al*., 1998). To test the relative influence of the nucleic acid binding NC domain and of the two spacer peptides on the assembly phenotype, we constructed expression vectors pET ΔMA-CA-NC and pET ΔMA-CA-NC(ΔSP1), encoding Gag-derived proteins lacking SP2 or both spacer peptides, respectively (Figure 6). Both proteins were purified to near homogeneity (Figure 6, right panels), dialyzed against either pH 8 or 6 buffer in the presence of nucleic acid, and analyzed by negative stain EM. The result for ΔMA-CA-NC was the same as for ΔMA-CA-NC-SP2; regular spherical particles with a narrow size distribution were recovered at the high pH (Figure 6A), while long tubular and conical particles were formed at pH 6 (Figure 6B). In contrast, *in vitro* assembly of ΔMA-CA-NC(ΔSP1) did not yield any spherical particles, independent of the pH of the reaction. Short and heterogeneous particles were observed when dialysis was performed either against pH 8 (Figure 6C) or pH 6 buffer (Figure 6D). Some cones and short tubes, resembling the particles observed for ΔMA-CA-NC at the lower pH (Figure 6B), were also found for ΔMA-CA-NC(ΔSP1). However, particle shape was generally significantly more heterogeneous in this case.

Previous studies had shown that some Gag-derived proteins can form particles resembling their respective *in vitro* assembly products inside bacterial cells (Klikova *et al*., 1995; Campbell and Vogt, 1997; Gross *et al*., 1998). We therefore analyzed the capacity of ΔMA-CA-NC and ΔMA-CA-NC(ΔSP1) to form ordered structures *in vivo* by thin section EM analysis of induced *E.coli* cells. These experiments showed that ΔMA-CA-NC formed homogeneous spherical particles of ~100 nm diameter in *E.coli* (Figure 7A), while ΔMA-CA-NC(ΔSP1) formed exclusively long helically arranged tubes (Figure 7B). In contrast to the *in vitro* assembly experiments, there was no difference in the morphology of cylinders derived from CA-NC or ΔMA-CA-NC(ΔSP1), but less particles were observed in the latter case. Immunoblot analysis of induced bacteria revealed that all proteins had the expected size (data not shown), confirming that the assembly phenotype was not due to proteolytic removal of domains. Taken together, these results suggest that SP1 is required for assembly of homogeneous spherical particles *in vitro* and

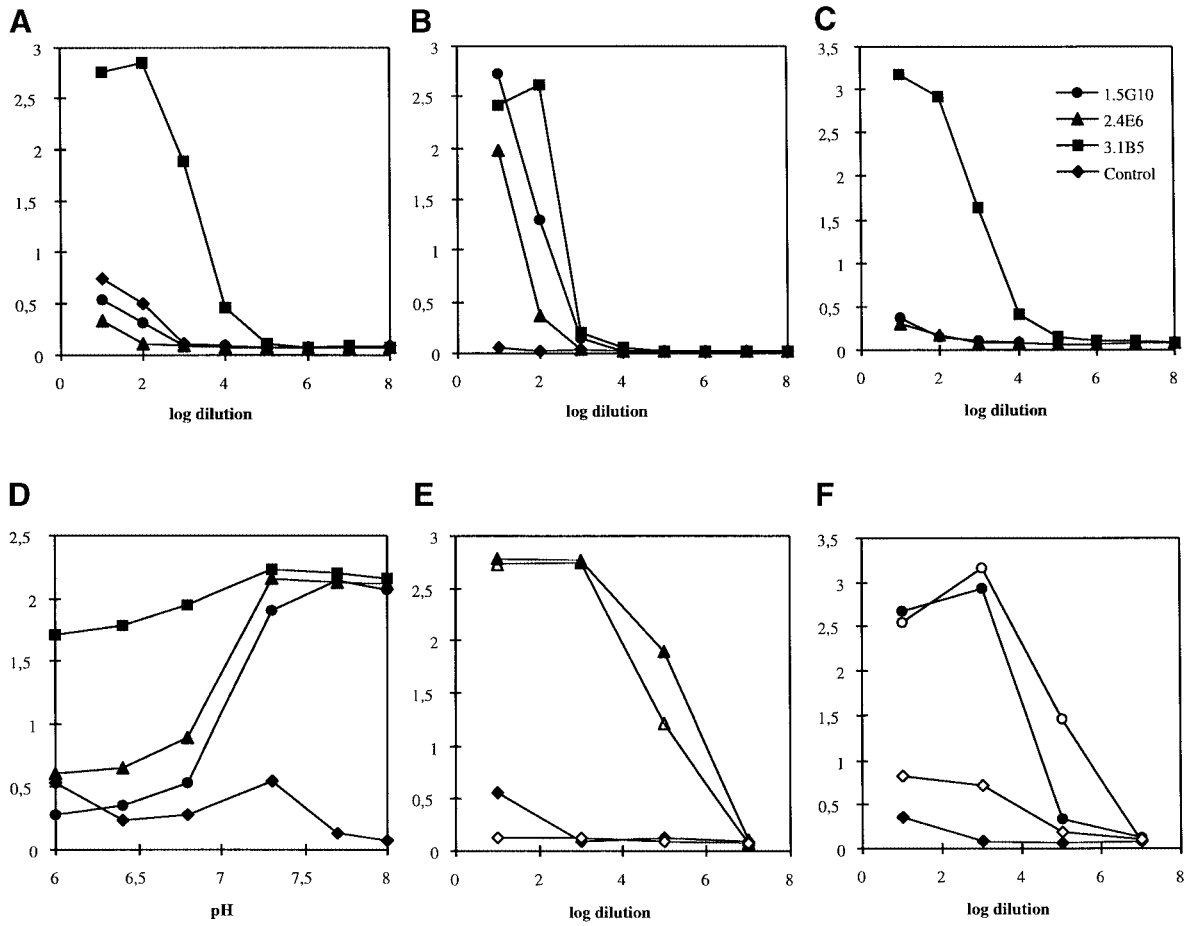

Fig. 5. Analysis of pH-dependent conformational changes using mAbs. Titration curves show binding of purified ΔMA-CA-NC-SP2 (**A**–**D**) or of CA-derived peptides (**E** and **F**) to HIV-1 CA-specific mAbs 1.5G10 (circles), 2.4E6 (triangles), 3.1B5 (squares), or a control antibody recognizing an irrelevant antigen (rhombuses). (A) Binding was performed at pH 6.0, (B) pH 8.0 and (C) pH 6.0 following preincubation of the protein at pH 8.0. The pH profile of antibody binding was analyzed in (D) over a pH range 6.0–8.0. Antibody dilution was 10^{-1} in this case. Titration curves in (E) and (F) show binding of mAbs 2.4E6 (E) and 1.5G10 (F) at pH 6.0 (filled symbols) and pH 8.0 (open symbols) to their respective peptide epitopes (2.4E6: amino acids 49–61 of CA; 1.5G10: amino acids 109–120 of CA).

in *E.coli* cells. Smaller heterogeneous spheres had been found when ΔMA-CA (Gross *et al*., 1998) or ΔMA-CA-SP1 (data not shown) were used for *in vitro* assembly, but not in *E.coli*, indicating that the NC domain and its interaction with nucleic acid are also important for regular sphere assembly.

Discussion

We have developed a system that allows the formation of spherical as well as tubular and conical particles from the same HIV-1 Gag-derived protein *in vitro*. Negative stain and thin section EM confirmed that the particles closely resemble immature and mature HIV-1 cores, respectively. *In vitro* assembly of Gag-derived particles with morphological likeness to immature retroviruses has been described for Rous sarcoma virus (Campbell and Vogt, 1997) and Mason Pfizer monkey virus (Klikova *et al*., 1995), but HIV-1 Gag-derived proteins yielded only spheres that were significantly smaller than authentic immature cores and often heterogeneous in size (Gross *et al*., 1998; von Schwedler *et al*., 1998; Campbell and Rein, 1999). As we show here using cryo-EM analysis, spherical particles generated from ΔMA-CA-NC-SP2 are not only similar to the immature virion in size and shape, but display a virtually identical inner organization.

The particles are formed from purified protein and oligodeoxynucleotides alone, demonstrating that cellular factors or other viral proteins are not required. Previously, we had shown that deletion of amino acids 16–99 within MA did not alter the morphology of virions produced in tissue culture (Fäcke *et al*., 1993). The analogous result is observed *in vitro*. The presence of this region even seems to inhibit important interactions *in vitro*, since a Gag-derived protein containing the complete MA domain formed only small spherical particles with a diameter of 25–30 nm *in vitro* (Campbell and Rein, 1999). In infected cells, interactions with cellular proteins or membranes may influence the assembly potential of HIV-1 Gag. Accordingly, addition of reticulocyte lysate altered the size distribution of particles formed from wild-type MA-CA-NC *in vitro* (Campbell and Rein, 1999). HIV-1 MA has been shown to bind to several cellular proteins (Lama and Trono, 1998; Cimarelli and Luban, 1999; Peytavi *et al*., 1999), but the relevance of these MA-interacting proteins for HIV-1 assembly and maturation remains unclear. Besides the MA globular domain, ΔMA-CA-NC lacks the p6 domain of the Gag precursor. The finding

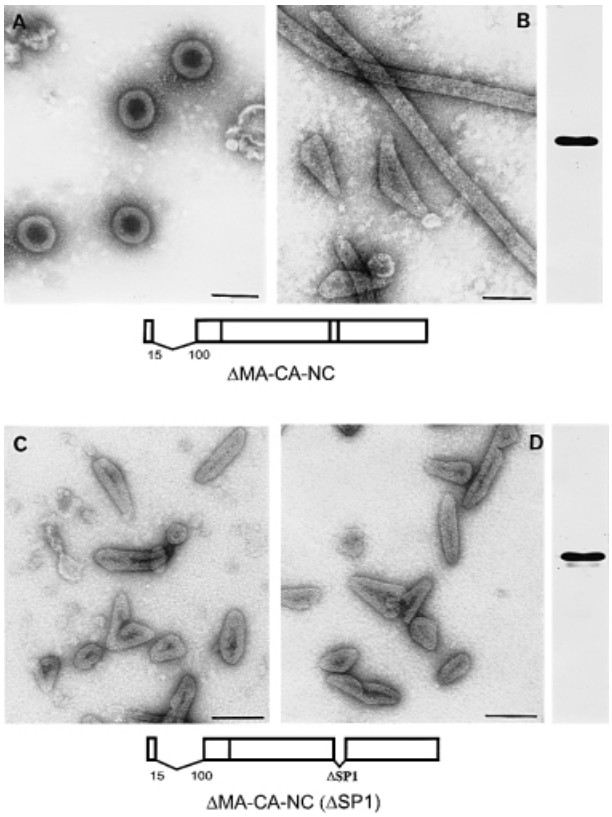

Fig. 6. Influence of SP1 on the *in vitro* assembly properties of ΔMA-CA-NC. Assembly of ΔMA-CA-NC (**A** and **B**) and ΔMA-CA-NC(ΔSP1) (**C** and **D**) was performed by dialysis against pH 8.0 (A and C) or pH 6.0 (B and D) buffer as described in Figure 2. Assembly products were concentrated and analyzed by negative stain EM. Analysis of purified proteins (2 μg each) on a Coomassie Blue-stained SDS–polyacrylamide gel is shown on the right. Bar, 100 nm.

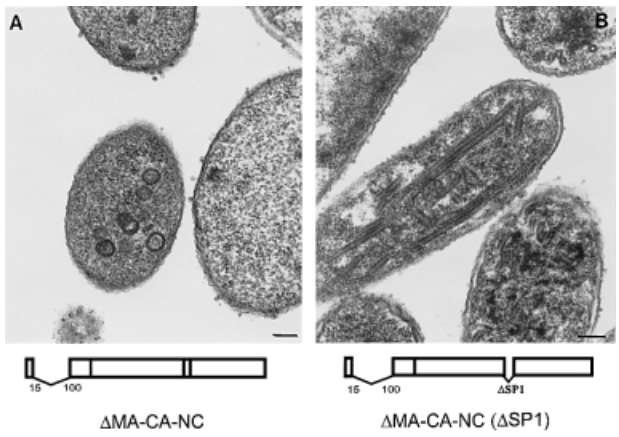

Fig. 7. Assembly properties of HIV-1 Gag-derived proteins in bacterial cells. *Escherichia coli* BL21 DE3 cells carrying the plasmids indicated were induced for 3 h and analyzed by ultrathin section EM in capillary tubes. Bar, 100 nm.

that this protein assembles into properly sized spherical particles *in vitro* argues against the suggested role for p6 in controlling particle size (Garnier *et al*., 1998). This discrepancy may be due to cellular factors binding to p6 during virion budding, which does not occur in the *in vitro* system.

Assembly experiments at different buffer conditions showed that the same protein is capable of forming either spherical or tubular and conical particles *in vitro*, depending on the pH of the reaction. Originally, it had been assumed that any N-terminal extension of HIV-1 CA would abolish tube formation, and it was proposed that the proteolytic liberation of Pro1 of CA followed by the formation of a salt bridge between Pro1 and Asp51 is a crucial conformational switch required for formation of tubular particles or mature HIV-1 cores (von Schwedler *et al*., 1998). Our finding that a CA protein bearing an additional 48 residues at its N-terminus can assemble into tubes shows that there is no absolute requirement for this salt bridge in assembly but does not argue against a role for it in virion maturation.

Assembly of regular particles of different morphologies has been described for a number of icosahedral viruses. While neither immature nor mature retroviral capsids display icosahedral symmetry (Fuller *et al*., 1997; Yeager *et al*., 1998), similar concepts of the systematic modulation of contacts between identical proteins must apply. Formation of particles of alternate shape can occur by using a subset of the interactions observed in the wild-type virion (Erickson *et al*., 1985). Alternatively, rearrangement of a localized portion of the structure against the background of an unchanging core may occur as in the case of cowpea chlorotic mottle virus and polyomaviruses, which form icosahedral particles of different size as well as long tubes (Bancroft, 1970; Salunke *et al*., 1986).

Our results identify two regions within the HIV-1 Gag polyprotein, which play a role in a conformational transition associated with assembly of tubes or spheres: the SP1 region downstream of CA (see below) and two helices in the N-terminal segment of CA. The latter region was identified by changes in the affinity of two mAbs to the Gag-derived protein, which occurred over the same pH range as the 'morphological switch'. Since the epitopes recognized by these mAbs have been mapped, we can localize regions of conformational alterations to amino acids 49–61 and 109–120 in CA, corresponding to helix 3 and helix 6 in the three-dimensional structure of the CA N-terminal domain (Gamble *et al*., 1996; Gitti *et al*., 1996). The conformational change either involves the epitopes themselves or shifts of neighboring structural elements render the epitope inaccessible, but no major structural rearrangements were observed. Recently, the structure of the CA N-terminal domain extended at its N-terminus by 4 amino acids has been determined by NMR analysis. The major difference in this structure compared with the N-terminal CA domain alone is a very significant shift of the position of helix 6. Helix 3 appears to be in a slightly different position as well and its packing is clearly different, because the salt bridge of Pro1 with Asp51 is not formed leading to a different interaction of helix 3 with the N-terminal β-hairpin (W.Sundquist, personal communication).

The conformational change occurs around pH 7, indicating that both conformers are presumably in equilibrium at close to physiological conditions. In *E.coli*, the protein formed only spherical particles, analogous to the Gag polyprotein *in vivo* and this may be explained by the intracellular pH being well above 7. Conformational transitions *in vitro* resulted from changing the buffer conditions, but we consider it unlikely that a pH shift plays a role in HIV maturation *in vivo*. Molecular events

triggered by a variation in pH may mimic alterations in inter- or intramolecular interactions resulting from proteolytic cleavage between Gag domains. However, the finding that the conformational change can be induced by a pH shift suggests that one or more titratable residues are involved. Normally, histidines would be expected to be affected in the pH 6–8 range, but the structure of the CA N-terminal domain shows that no conserved His residues are part of or interact with the epitopes recognized by the mAbs. Other titratable residues should also be considered, since the local environment can greatly influence their pKa. Precedents for morphological changes around neutral pH involving acidic residues do exist in other viral systems (Johnson, 1996). There are several highly conserved acidic residues in HIV-1 CA and two of them (E113 and D51, the latter being invariant among retroviruses and involved in the described N-terminal salt bridge) are part of the recognized epitopes. However, in the absence of structural information on larger assemblies, the influence of the local environment on these residues in the HIV-1 capsid cannot be predicted.

The SP1 deletion variant ΔMA-CA-NC(ΔSP1) assembles into heterogeneous cones and short tubes, but is no longer capable of sphere formation. Based on computational modeling it has been postulated that SP1 forms an α-helix together with the C-terminal residues of CA, which are not resolved in the crystal structure (Accola *et al*., 1998). Proteolytic separation of CA and SP1 would destroy the proposed helix and allow a rearrangement of the CA C-terminus necessary for maturation. When processing between CA and SP1 is inhibited by mutagenesis at the protease cleavage site, virus particles are released but capsid condensation is inhibited and a roughly spherical CA layer separated from the virion membrane is observed without a cone-shaped capsid shell (Accola *et al*., 1998; Wiegers *et al*., 1998). Conceivably, the presence of SP1 prevents CA from adopting its 'mature' conformation and arrests the CA layer in the position it occupied in the immature virion, even though the N-terminal MA and C-terminal NC-p6 regions have been removed. The presence of SP1, on the other hand, is essential for assembly of regular immature virions in tissue culture and deletion of SP1 or mutation of conserved residues severely affected particle formation. Instead of budding virions, large electron-dense plaques, sometimes curled up at the ends, were found underneath the plasma membrane (Kräusslich *et al*., 1995; Accola *et al*., 1998). The interactions between Gag molecules within the protein sheets may be analogous to those between ΔMA-CA-NC molecules in the cylindrical particles. In tissue culture, the association of the MA domain with the plasma membrane might prevent a helical arrangement of Gag molecules and lead to a spreading of the protein into flat membrane-bound arrays. The data obtained in the viral context agree with the proposition of SP1 being a morphological switch region. However, the finding that a protein comprising only CA and SP1 (CA+14) does not assemble into spheres *in vitro* but forms cylinders instead (Gross *et al*., 1997) indicates that SP1 is not the sole determinant of particle morphology. Sequential rearrangements within the N- and C-terminal domains of CA may be important and both domains may interact with each other in the process of capsid maturation. In summary, we propose that assembly of the immature HIV-1 capsid requires a continuous assembly domain that spans the C-terminus of CA, SP1 and NC as well as N-terminal extension of CA. Two distinct switches function during maturation: cleavage between MA and CA leads to formation of the N-terminal salt bridge and consequent rearrangement of the N-terminus of CA without changing the localization of CA in the particle. Subsequent removal of SP1 triggers capsid condensation.

Materials and methods

Expression plasmids

All plasmids are derived from the prokaryotic expression vectors pET11c and pET3c (Novagen, Madison, WI), which carry a T7 expression cassette. Plasmid pET ΔMA-CA-NC-SP2 (Figure 1) was constructed by inserting the *Nde*I–*Spe*I fragment from pET ΔMA-CA (Gross *et al*., 1998) into pET HIV CA-NC (Campbell and Vogt, 1995), which had been opened with the same enzymes. Because pET HIV CA-NC was derived from the BH10 strain of HIV-1 (Ratner *et al*., 1987), this plasmid contains BH10 sequences from the *Spe*I site to the 3′ end. Plasmid pET ΔMA-CA-NC, lacking SP2 sequences, was constructed by inserting the *Nde*I–*Spe*I fragment from pET ΔMA-CA into pET CA-NC (Gross *et al*., 1997), which is derived from the HIV-1 strain NL4-3 (Adachi *et al*., 1986). The derivative pET ΔMA-CA-NC(ΔSP1) was made by exchanging the *Spe*I–*Apa*I (nt 1507–2006 of HIV-1 strain NL4-3) fragment of this plasmid for that of pNL43-CA3 (Kräusslich *et al*., 1995), thereby introducing a deletion of the 14 codons of SP1. The HIV-specific regions were verified by sequence analysis.

Expression and purification of recombinant proteins

Induction of *E.coli* BL21 DE3 cells was performed as described (Gross *et al*., 1997). Bacterial cells were resuspended in cold lysis buffer [50 mM Tris–HCl pH 8.5, 1 mM EDTA, 5 mM dithiothreitol (DTT), 1 M LiCl] and disrupted by disintegration using glass beads and subsequent sonication. After centrifugation at 27 000 *g* for 10 min, proteins were precipitated from the soluble fraction by addition of ammonium sulfate to 25% saturation, redissolved in buffer containing 50 mM Tris–HCl pH 8.3, 0.5 M NaCl, 1 mM EDTA and 1 mM DTT and nucleic acids were removed by anion exchange chromatography using a POROS HQ 20/M anion exchange column (PerSeptive Biosystems) equilibrated with the same buffer. Proteins were collected from the unbound material by ammonium sulfate precipitation and redissolved in a buffer containing 50 mM 2-(*N*-morpholino) ethane sulfonic acid (MES) pH 6.0, 0.5 M NaCl, 1 mM EDTA and 1 mM DTT. After dilution to a salt concentration of 200 mM NaCl, the material was further purified on a POROS SP 20/M cation exchange column. Purified proteins were collected by ammonium sulfate precipitation, redissolved to a concentration of 3–10 mg/ml in 30 mM MES pH 6.0, 1 mM EDTA, 1 mM DTT, 0.5 M NaCl and stored at –70°C.

Virus-like particles were produced using the recombinant baculovirus AcNPVgag12myr (Royer *et al*., 1991) in Sf21 insect cells. Particles were harvested from the cell culture medium and collected by ultracentrifugation through a cushion of 20% (w/w) sucrose.

Analysis of expression products

Protein samples were separated on 17.5% SDS–polyacrylamide gels (ratio 200:1 of acrylamide to *N*,*N*-methylenebisacrylamide) and stained with Coomassie Blue. Protein concentration was determined according to Gill and von Hippel (1989).

In vitro assembly

Protein stock solutions were diluted to the appropriate concentration (2 mg/ml unless stated otherwise) with storage buffer (30 mM MES pH 6.0, 1 mM EDTA, 1 mM DTT, 0.5 M NaCl) and dialyzed for 2 h at 4°C against the assembly buffer indicated (50 mM Tris–HCl pH 8.0, 7.5 or 7.0 or 50 mM MES pH 6.0 or 6.5, always containing 0.1 M NaCl, 1 mM EDTA and 1 mM DTT) in the presence of nucleic acid (total *E.coli* RNA, bacteriophage MS2 RNA, single-stranded M13-DNA or single-stranded DNA oligonucleotides). Oligodeoxynucleotides were between 12 and 92 bases in length and had been originally made for various cloning projects. Sequences of oligodeoxynucleotides are available upon request. The concentration of nucleic acid was 5% (by weight) of protein unless stated otherwise.

Electron microscopy analysis

For negative staining of *in vitro* assembly products, 5 μl samples of dialyzed protein solutions or of the resuspended pellet after concentration in the

microcentrifuge were applied on parafilm and covered with a UV-irradiated Formvar/carbon-coated grid (mesh size 200) for 5 min. Subsequently, the grid was applied to a drop of uranyl acetate for 5 min. Excess stain was blotted off with filter paper, and the grid was air dried and analyzed using a Philips CM 120 transmission electron microscope at 80 kV.

For ultrathin section EM analysis of *in vitro* assembly products, particles were concentrated by centrifugation for 5 min in the microcentrifuge, and the concentrated suspension was drawn into cellulose capillary tubes by capillary action as described (Hohenberg *et al*., 1994). Subsequently, assembly products were fixed within the capillaries for 20 min with 2.5% glutaraldehyde in phosphate-buffered saline (PBS), post-fixed for 30 min with 1% OsO_4 in PBS, washed with water, stained for 30 min in 1% uranyl acetate in water and dehydrated in a graded series of ethanol. Capillary tubes were embedded in ERL resin for ultramicrotomy. Sections were counterstained with 2% uranyl acetate and lead citrate.

For EM analysis of induced *E.coli*, bacteria were collected by brief centrifugation, fixed in 4% paraformaldehyde and 2% glutaraldehyde in PBS for 5 min on ice, washed with PBS and collected by brief centrifugation. Subsequently, the wet bacterial paste was drawn into capillary tubes and bacterial cells were post-fixed, and further processed within the capillaries as described above.

Cryo-electron microscopy

In vitro assembly products were collected by 5 min centrifugation, resuspended in 1/4 of the original volume, and 4 µl were applied to holey carbon films on copper grids at room temperature. Then, in order to lower the salt concentration of the specimen, grids were placed on drops of distilled water for ~20 s with the sample side pointing up. Excess water was blotted off with filter paper and the specimen was vitrified by plunging the grid into liquid ethane, which was cooled by liquid nitrogen. The specimen was loaded in a Gatan 656 cryoholder cooled by liquid nitrogen to –180°C. Images were recorded on a Philips CM200 with a field emission gun operated at 200 kV. Low dose conditions (5–10 $e^-/Å^2$) were used at a magnification of 38 000 and a defocus of approximately –1.5 µm. Images were digitized with a Zeiss SCAI scanner at a raster of 14 µm resulting in a nominal sampling of 3.62 Å per pixel.

Preparation of monoclonal antibodies and ELISA

Preparation of mAbs will be described elsewhere. Briefly, mice were immunized with purified ΔMA-CA protein and spleen cells were fused to Sp2/0 (1.5G10, 3.1B5) or NS-1 myeloma cells (2.4E6) using standard protocols. Hybridomas were screened against purified HIV-1 CA protein and against delipidated Gag particles. Epitope mapping was performed by ELISA using a set of overlapping 24mer peptides corresponding to the entire CA sequence (Haist *et al*., 1992). For antibody production, cells were either propagated in stationary cultures or in minifermenters (MiniPerm, InVitro Systems, Hanau, Germany).

A panel of 12 CA-reactive mAbs was analyzed by ELISA for binding of ΔMA-CA-NC-SP2. Protein (2 µg/ml) or peptide (4 µg/ml) antigen was incubated overnight with hybridoma culture supernatant serially diluted either in 30 mM MES pH 6.0, 0.1 M NaCl, or in 30 mM Tris–HCl pH 8.0, 0.1 M NaCl in a standard microtiter plate. The mixture was then transferred to a second plate (MaxiSorb, Nunc, Germany) that had been coated with polyclonal rabbit-anti HIV-1 CA (1 µg/ml) and blocked with 10% newborn calf serum. Incubation with the antigen–antibody mixture was for 3 h at room temperature, bound mouse antibodies were detected by incubation with peroxidase-conjugated anti-mouse immunoglobulins (Jackson Laboratories) for 1 h at 37°C. Color was developed in sodium citrate buffer at pH 5 using 1,2-phenylenediamine as chromogen. All wash steps were performed using buffers of the appropriate pH containing 0.05% Tween-20. For a more precise determination of the pH effect, ELISA experiments were performed as described above using the following buffers: 30 mM MES at pH 6.0, 6.4 or 6.8; 30 mM Tris–HCl at pH 7.3, 7.7 and 8.0. All buffers contained 0.1 M NaCl. Wash steps were performed using the same buffer containing 0.05% Tween-20.

Acknowledgements

We are grateful to Wes Sundquist for communicating results prior to publication, to S.Modrow for the set of overlapping peptides, and to S.Campbell and V.Vogt for plasmid pET HIV CA-NC. We thank R.Jaenicke for making the CD-spectropolarimeter available and V.Vogt for helpful discussion. This work was supported in part by grants from the Deutsche Forschungsgemeinschaft to H.-G.K. and S.F.

References

Accola,M.A., Höglund,S. and Göttlinger,H.G. (1998) A putative α-helical structure which overlaps the capsid-p2 boundary in the human immunodeficiency virus type 1 Gag precursor is crucial for viral particle assembly. *J. Virol.*, **72**, 2072–2078.

Adachi,A., Gendelman,H.E., Koenig,S., Folks,T., Willey,R., Rabson,A. and Martin,M.A. (1986) Production of acquired immunodeficiency syndrome-associated retrovirus in human and nonhuman cells transfected with an infectious molecular clone. *J. Virol.*, **59**, 284–291.

Bancroft,J.B. (1970) The self-assembly of spherical plant viruses. *Adv. Virus Res*., **16**, 99–134.

Berthet-Colominas,C., Monaco,S., Novelli,A., Sibai,G., Mallet,F. and Cusack,S. (1999) Head-to-tail dimers and interdomain flexibility revealed by the crystal structure of HIV-1 capsid protein (p24) complexed with a monoclonal antibody Fab. *EMBO J*., **18**, 1124–1136.

Campbell,S. and Rein,A. (1999) *In vitro* assembly properties of human immunodeficiency virus type 1 Gag protein lacking the p6 domain. *J. Virol.*, **73**, 2270–2279.

Campbell,S. and Vogt,V.M. (1995) Self-assembly *in vitro* of purified CA-NC proteins from Rous sarcoma virus and human immunodeficiency virus type 1. *J. Virol.*, **69**, 6487–6497.

Campbell,S. and Vogt,V.M. (1997) *In vitro* assembly of virus-like particles with Rous sarcoma virus Gag deletion mutants: identification of the p10 domain as a morphological determinant in the formation of spherical particles. *J. Virol.*, **71**, 4425–4435.

Cimarelli,A. and Luban,J. (1999) Translation elongation factor 1-α interacts specifically with the human immunodeficiency virus type 1 Gag polyprotein. *J. Virol.*, **73**, 5388–5401.

De Guzman,R.N., Wu,Z.R., Stalling,C.C., Pappalardo,L., Borer,P.N. and Summers,M.F. (1998) Structure of the HIV-1 nucleocapsid protein bound to the SL3 ψ-RNA recognition element. *Science*, **279**, 384–388.

Erickson,J.W., Silva,A.M., Murthy,M.R., Fita,I. and Rossmann,M.G. (1985) The structure of a T = 1 icosahedral empty particle from southern bean mosaic virus. *Science*, **229**, 625–629.

Fäcke,M., Janetzko,A., Shoeman,R.L. and Kräusslich,H.G. (1993) A large deletion in the matrix domain of the human immunodeficiency virus gag gene redirects virus particle assembly from the plasma membrane to the endoplasmic reticulum. *J. Virol.*, **67**, 4972–4980.

Fuller,S.D., Wilk,T., Gowen,B.E., Kräusslich,H.G. and Vogt,V.M. (1997) Cryo-electron microscopy reveals ordered domains in the immature HIV-1 particle. *Curr. Biol.*, **7**, 729–738.

Gamble,T.R., Vajdos,F.F., Yoo,S., Worthylake,D.K., Houseweart,M., Sundquist,W.I. and Hill,C.P. (1996) Crystal structure of human cyclophilin A bound to the amino-terminal domain of HIV-1 capsid. *Cell*, **87**, 1285–1294.

Gamble,T.R., Yoo,S., Vajdos,F.F., von Schwedler,U.K., Worthylake,D.K., Wang,H., McCutcheon,J.P., Sundquist,W.I. and Hill,C.P. (1997) Structure of the carboxyl-terminal dimerization domain of the HIV-1 capsid protein. *Science*, **278**, 849–853.

Ganser,B.K., Li,S., Klishko,V.Y., Finch,J.T. and Sundquist,W.I. (1999) Assembly and analysis of conical models for the HIV-1 core. *Science*, **283**, 80–83.

Garnier,L., Ratner,L., Rovinski,B., Cao,S.X. and Wills,J.W. (1998) Particle size determinants in the human immunodeficiency virus type 1 Gag protein. *J. Virol.*, **72**, 4667–4677.

Gheysen,D., Jacobs,E., de Foresta,F., Thiriart,C., Francotte,M., Thines,D. and De Wilde,M. (1989) Assembly and release of HIV-1 precursor Pr55gag virus-like particles from recombinant baculovirus-infected insect cells. *Cell*, **59**, 103–112.

Gill,S.C. and von Hippel,P.H. (1989) Calculation of protein extinction coefficients from amino acid sequence data. *Anal. Biochem*., **182**, 319–326.

Gitti,R.K., Lee,B.M., Walker,J., Summers,M.F., Yoo,S. and Sundquist,W.I. (1996) Structure of the amino-terminal core domain of the HIV-1 capsid protein. *Science*, **273**, 231–235.

Gross,I., Hohenberg,H. and Kräusslich,H.G. (1997) *In vitro* assembly properties of purified bacterially expressed capsid proteins of human immunodeficiency virus. *Eur. J. Biochem*., **249**, 592–600.

Gross,I., Hohenberg,H., Huckhagel,C. and Kräusslich,H.G. (1998) N-terminal extension of human immunodeficiency virus capsid protein converts the *in vitro* assembly phenotype from tubular to spherical particles. *J. Virol.*, **72**, 4798–4810.

Haist,S., Marz,J., Wolf,H. and Modrow,S. (1992) Reactivities of HIV-1 gag-derived peptides with antibodies of HIV-1-infected and uninfected humans. *AIDS Res. Hum. Retroviruses*, **8**, 1909–1917.

Henderson,L.E., Sowder,R.C., Copeland,T.D., Oroszlan,S. and Benveniste,R.E. (1990) Gag precursors of HIV and SIV are cleaved into six proteins found in the mature virions. *J. Med. Primatol*., **19**, 411–419.

Hohenberg,H., Mannweiler,K. and Müller,M. (1994) High-pressure freezing of cell suspensions in cellulose capillary tubes. *J. Microsc*., **175**, 34–43.

Johnson,J.E. (1996) Functional implications of protein–protein interactions in icosahedral viruses. *Proc. Natl Acad. Sci. USA*, **93**, 27–33.

Johnson,J.E. and Speir,J.A. (1997) Quasi-equivalent viruses: a paradigm for protein assemblies. *J. Mol. Biol.*, **269**, 665–675.

Klikova,M., Rhee,S.S., Hunter,E. and Ruml,T. (1995) Efficient *in vivo* and *in vitro* assembly of retroviral capsids from Gag precursor proteins expressed in bacteria. *J. Virol.*, **69**, 1093–1098.

Kräusslich,H.G., Fäcke,M., Heuser,A.M., Konvalinka,J. and Zentgraf,H. (1995) The spacer peptide between human immunodeficiency virus capsid and nucleocapsid proteins is essential for ordered assembly and viral infectivity. *J. Virol.*, **69**, 3407–3419.

Lama,J. and Trono,D. (1998) Human immunodeficiency virus type 1 matrix protein interacts with cellular protein HO3. *J. Virol.*, **72**, 1671–1676.

Liddington,R.C., Yan,Y., Moulai,J., Sahli,R., Benjamin,T.L. and Harrison,S.C. (1991) Structure of simian virus 40 at 3.8-Å resolution. *Nature*, **354**, 278–284.

Massiah,M.A., Starich,M.R., Paschall,C., Summers,M.F., Christensen,A.M. and Sundquist,W.I. (1994) Three-dimensional structure of the human immunodeficiency virus type 1 matrix protein. *J. Mol. Biol.*, **244**, 198–223.

Matthews,S., Barlow,P., Clark,N., Kingsman,S., Kingsman,A. and Campbell,I. (1995) Refined solution structure of p17, the HIV matrix protein. *Biochem. Soc. Trans*., **23**, 725–729.

Momany,C. *et al*. (1996) Crystal structure of dimeric HIV-1 capsid protein. *Nature Struct. Biol.*, **3**, 763–770.

Nermut,M.V. and Hockley,D.J. (1996) Comparative morphology and structural classification of retroviruses. *Curr. Top. Microbiol. Immunol.*, **214**, 1–24.

Peytavi,R., Hong,S.S., Gay,B., d'Angeac,A.D., Selig,L., Benichou,S., Benarous,R. and Boulanger,P. (1999) HEED, the product of the human homolog of the murine *eed* gene, binds to the matrix protein of HIV-1. *J. Biol. Chem.*, **274**, 1635–1645.

Prasad,B.V., Prevelige,P.E., Marietta,E., Chen,R.O., Thomas,D., King,J. and Chiu,W. (1993) Three-dimensional transformation of capsids associated with genome packaging in a bacterial virus. *J. Mol. Biol.*, **231**, 65–74.

Prevelige,P.E.,Jr, Thomas,D., Aubrey,K.L., Towse,S.A. and Thomas,G.J.,Jr (1993) Subunit conformational changes accompanying bacteriophage P22 capsid maturation. *Biochemistry*, **32**, 537–543.

Ratner,L., Fisher,A., Jagodzinski,L.L., Mitsuya,H., Liou,R.S., Gallo,R.C. and Wong-Staal,F. (1987) Complete nucleotide sequences of functional clones of the AIDS virus. *AIDS Res. Hum. Retroviruses*, **3**, 57–69.

Royer,M., Cerutti,M., Gay,B., Hong,S.S., Devauchelle,G. and Boulanger,P. (1991) Functional domains of HIV-1 gag-polyprotein expressed in baculovirus-infected cells. *Virology*, **184**, 417–422.

Salunke,D.M., Caspar,D.L. and Garcea,R.L. (1986) Self-assembly of purified polyomavirus capsid protein VP1. *Cell*, **46**, 895–904.

von Schwedler,U.K., Stemmler,T.L., Klishko,V.Y., Li,S., Albertine,K.H., Davis,D.R. and Sundquist,W.I. (1998) Proteolytic refolding of the HIV-1 capsid protein amino-terminus facilitates viral core assembly. *EMBO J*., **17**, 1555–1568.

Wiegers,K., Rutter,G., Kottler,H., Tessmer,U., Hohenberg,H. and Kräusslich,H.G. (1998) Sequential steps in human immunodeficiency virus particle maturation revealed by alterations of individual Gag polyprotein cleavage sites. *J. Virol.*, **72**, 2846–2854.

Wilk,T. and Fuller,S.D. (1999) Towards the structure of the human immunodeficiency virus: divide and conquer. *Curr. Opin. Struct. Biol.*, **9**, 231–243.

Worthylake,D.K., Wang,H., Yoo,S., Sundquist,W.I. and Hill,C.P. (1999) Structures of the HIV-1 capsid protein dimerization domain at 2.6 Å resolution. *Acta Crystallogr. D*, **55**, 85–92.

Yeager,M., Wilson-Kubalek,E.M., Weiner,S.G., Brown,P.O. and Rein,A. (1998) Supramolecular organization of immature and mature murine leukemia virus revealed by electron cryo-microscopy: implications for retroviral assembly mechanisms. *Proc. Natl Acad. Sci. USA*, **95**, 7299–7304.

Received September 28, 1999; revised November 8, 1999; accepted November 10, 1999